




Novel plant-derived compounds modulate gut microbiome dysbiosis in colitis mice: A potential therapeutic avenue for inflammatory bowel disease

Md. Mizanur Rahaman^{a,b}, Karma Yeshe^c, Mehedi Hasan Bappi^d, Md. Zohorul Islam^e,
Phurpa Wangchuk^{c,f,1}, Subir Sarker^{a,b,g,1,*} 

^a Biomedical Sciences and Molecular Biology, College of Medicine and Dentistry, James Cook University, Townsville, QLD 4811, Australia

^b Australian Institute of Tropical Health and Medicine, James Cook University, Townsville, QLD 4811, Australia

^c College of Science and Engineering, James Cook University, Nguma Bada campus, McGregor Rd, Smithfield, Cairns, QLD 4878, Australia

^d School of Pharmacy, Jeonbuk National University, Jeonju 54896, Republic of Korea

^e CSIRO Health & Biosecurity, Australian Centre for Disease Preparedness, Geelong, Victoria, Australia

^f Australian Institute of Tropical Health and Medicine, James Cook University, Nguma Bada campus, McGregor Rd, Smithfield, Cairns, QLD 4878, Australia

^g Department of Microbiology, Anatomy, Physiology and Pharmacology, School of Agriculture, Biomedicine and Environment, La Trobe University, Melbourne, Victoria 3086, Australia

ARTICLE INFO

Keywords:

IBD
Microbiome
Dysbiosis
Galloyl-lawsoniaside A
Uromyrtoside
Dexamethasone

ABSTRACT

Inflammatory bowel disease (IBD) is a chronic, multifactorial disorder of the gastrointestinal tract, often associated with dysbiosis in gut microbiota. While the exact cause of IBD remains unclear, alterations in gut microbiome composition and function are recognised as key contributors to IBD pathogenesis. Natural compounds with anti-inflammatory properties are increasingly explored as potential therapeutic options for IBD. This study evaluated the therapeutic effects of two newly isolated galloyl glucosides—galloyl-lawsoniaside A (comp-4) and uromyrtoside (comp-6)—alongside dexamethasone (DEX) on microbiome regulation in a 2, 4, 6-Trinitrobenzene sulfonic acid (TNBS)-induced colitis mouse model. We employed PacBio HiFi full-length 16S rRNA gene sequencing on mouse colon tissue to assess changes in the intestinal microbiome and its associated functional pathways. TNBS-induced colitis significantly altered microbial composition, increasing the abundance of *Acetivibacter muris*, *Monoglobus pectinilyticus*, *Streptococcus pneumoniae*, *Parabacteroides merdae*, and *Haemophilus influenzae*, while decreasing *Staphylococcus ureilyticus* and *Mailhella massiliensis*. Treatment with comp-4 and 6 effectively restored the imbalanced microbiota. Functional pathway analysis revealed that colitis reduced microbial pathways, including peptidoglycan biosynthesis and the Bifidobacterium shunt. These disruptions were restored following treatment with our plant-derived compounds. Functional improvements were likely associated with reduced IL-6 production and restoring intestinal barrier integrity. Notably, comp-4 exhibited the most pronounced therapeutic efficacy across both microbial and host-associated parameters. *In silico* docking further supported the anti-inflammatory and immunomodulatory potential of these compounds. Together, our findings highlight the interplay between microbial function and host immunity in IBD and identify plant-derived galloyl glucosides as promising candidates for microbiome-targeted IBD therapeutics.

1. Introduction

Inflammatory bowel disease (IBD) is a chronic and recurrent disorder of the intestinal tract characterised by inflammation (Ritmejerlytė et al., 2022). IBD primarily manifests in two forms: ulcerative colitis and Crohn's disease, which differ in their clinical features, affected locations

of the gastrointestinal tract (Rahaman et al., 2025). Both conditions, however, are driven by a complex interplay of factors, including genetic predisposition, environmental influences, deregulated immune responses, and changes in gut microbiota. Despite advancements in understanding the exact combination of these factors leading to disease onset remains still unknown (Xavier and Podolsky, 2007; Torres et al.,

* Corresponding author at: Biomedical Sciences and Molecular Biology, College of Medicine and Dentistry, James Cook University, Townsville, QLD 4811, Australia

E-mail address: subir.sarker@jcu.edu.au (S. Sarker).

¹ Equally contributed as senior author.

<https://doi.org/10.1016/j.micres.2025.128343>

2017; Chang, 2020). Historically, IBD was thought to be primarily a Western illness, impacting over 1.4 million Americans (Loftus Jr and Sandborn, 2002). However, with the rise of industrialization, IBD has emerged as a global health concern, affecting millions of patients in both Western and Eastern hemispheres (Ng et al., 2017). In Australia, IBD has a considerable high prevalence. According to PricewaterhouseCoopers Australia (PwC), the estimated number of cases in 2018 ranged from 75,302 to 92,571, reflecting a significant upward trend in incidence (Health, 2019). The healthcare costs for patients with IBD are significantly higher compared to those without this condition. The annual expenditure on IBD treatment is estimated at approximately AU \$100 million for hospitalizations in Australia, with over AU \$380 million is lost due to reduced productivity, along with an estimated AU \$2.7 billion in other financial and economic expenses associated with IBD (Yeshi et al., 2020).

The rise in IBD infection is partly attributable to lack of treatment and definite understanding of the causes of the disease. Epidemiological research has suggested that human gut microbiome play significant role in IBD pathogenesis. Gut microbiome is a complex ecosystem of microorganisms, including bacteria, viruses, fungi, and archaea that works together with human body to maintain the balance (Zhang et al., 2024). This relationship is essential for maintaining homeostasis in the gastrointestinal tract, where gut microbiota play a crucial role in protecting the gut epithelial barrier, promoting drug and nutrient metabolism, and regulating the immune system (Weersma et al., 2020). Over the past decade, there has been a significant interest regarding the potential role of the gut microbiome in the development of IBD; particularly *Bacteroidetes* and *Firmicutes* whereas significant changes have been observed in the ratio of *Firmicutes* to *Bacteroidetes* during IBD (Zhao et al., 2022). However, this dysregulation of the gut microbiota can exacerbate inflammation by increasing intestinal permeability, facilitating the proliferation of pathogenic bacteria, and diminishing beneficial bacterial diversity (Huttenhower et al., 2014; Chang, 2020). Recent research has demonstrated that the balance between T regulatory (Treg) cells and T helper 17 (Th17) cells is critical in the development of IBD, indicating that this balance may represent a viable target for treatment (Waldschmitt et al., 2019). Furthermore, dysbiosis of the gut microbiota can disrupt the Treg/Th17 balance, thereby exacerbating inflammatory responses (Britton et al., 2019). Thus, maintaining the balance and functionality of the gut microbiome is crucial for intestinal health.

Despite the complex nature of IBD, current treatment options primarily on achieving remission, yet many patients experience relapse over time (Zhang et al., 2020). Consequently, there is an urgent need for improved therapeutic strategies to cure IBD. In this context, alternative treatments derived from natural products are increasingly being explored. These alternatives are particularly appealing because they tend to have fewer side effects compared to conventional therapies (Yeshi et al., 2024). Recent research has demonstrated that natural products may have therapeutic potential to treat diseases and improve gut health by altering the gut microbiota in animal models of dysbiosis (Wu and Tan, 2019). Plant-derived compounds, such as flavonoids and phenolic acids, have demonstrated anti-inflammatory effects and are known to influence the expression of key cytokines, including COX-2, TNF- α , NF- κ B, IL-1, IFN- γ , IL-8, IL-17A, IL-6, TGF- β , and IL-10 (Hur et al., 2012; Ihara et al., 2017; Ritmejerlytè et al., 2022). By modulating these cytokines, natural products may restore immune balance and reduce inflammation, making them promising agents for conditions linked to gut microbiota dysregulation and immune dysfunction.

To investigate the effects of plant-derived compounds on the gut microbiome associated with IBD, we investigated two novel plant comps 4 and 6 isolated from *Uromyrtus metrosideros* (F.M.Bailey) A.J.Scott. In a previous study, we investigated the anti-inflammatory properties of novel comps 4 and 6, where comp-4 showed significant suppression of interferon γ (IFN- γ), IL-17A, and IL-8 levels (Ritmejerlytè et al., 2022). However, the microbiome's role in the context of these compounds remained unexplored. Therefore, we aimed to characterize the gut

microbiome composition across naive, TNBS, and treatment groups (comp-4, comp-6 and standard drug-DEX) using full-length 16S rRNA sequencing. We also sought to elucidate the mechanisms by which these compounds influence the microbiome in the IBD setting.

2. Materials and methods

2.1. In-vivo animal trial and sample preparation

Colitis was induced in mice (Fig. 1) by administering an ethanolic solution of TNBS intrarectally (IR) as per the stated established method described by us previously for another study (Wangchuk et al., 2015). Before inducing colitis, mice were anaesthetised with 6.6 % ketamine and 0.6 % xylazine (obtained from Provect) in PBS by intraperitoneal (IP) injection. Subsequently, colitis was induced by intrarectal administration of 2.5 mg/100 μ l TNBS (Sigma) in 50 % ethanol under anaesthesia on day 0. On the following day, the TNBS induced mice were randomly assigned to one of three treatment groups, received individual treatments of 20 μ g of relevant compounds or standard/control drug-DEX in PBS by IP injection. Naive and 'TNBS' groups received an equal 200 μ l volume of solvents (DMSO and PBS) used for dissolving compounds or standard drug by IP injection.

A total of 50 mice were used in the experiment: naive (n = 10), TNBS (n = 10), DEX (n = 10), comp-4 (n = 10), and comp-6 (n = 10). Mice were monitored and scored daily for clinical symptoms as described previously for another study (Wangchuk et al., 2015). At the end of the experimental period, mice were euthanized according to ethical guidelines, and a midline laparotomy was performed to expose and remove the gut. The collected gut was rinsed with sterile saline to remove fecal content, then cut into small pieces (1–2 cm) and placed into sterile, labelled tubes. RNAlater was added to the tubes to preserve the tissue, which was then stored at -80°C for subsequently analyses.

2.2. Genomic DNA extraction and full-length 16S sequencing

Total genomic DNA from archived mouse colon samples was extracted using the DNeasy PowerSoil Pro Kit (Qiagen, Germany). While this kit is primarily used for soil and environmental samples, it was selected for this study based on its strong lysis capabilities for diverse microbial cell types and efficient removal of PCR inhibitors, features critical for complex gut microbiome samples (Song et al., 2021). Importantly, this kit is widely used for DNA extraction from faecal samples for microbiome study (Krigul et al., 2021; Knowler et al., 2023), which inherently contain sloughed gut epithelial cells and mucosa-associated microbiota. Based on this rationale, we extended its application to mouse gut tissue, as the microbial composition in gut scrapings closely resembles that of faecal material. To our knowledge, this is the first application of this kit for mouse gut tissue DNA extraction. We carefully validated the extracted DNA quality and quantity to ensure suitability for downstream applications, selecting samples with DNA concentrations > 50 ng/ μ l and optical density ratios (260/280 nm) between 1.8 and 2.0.

Briefly, mouse gut tissue was scraped using a sterile scalpel blade and transferred to an Eppendorf tube containing phosphate-buffered saline (PBS). A bead was added to each tube, and the samples were vortexed using a TissueLyser-LT2 (Qiagen, Germany) for approximately 10 min to ensure thorough tissue disruption. The samples were then centrifuged at 8000 g for 5 min, and the supernatant was used to extract genomic DNA, following the manufacturer's instructions. Primer selection and amplification of the full-length 16S rRNA gene (~1500 bp) for microbiome analysis were performed by the Australian Genome Research Facility (AGRF) in Brisbane using the universal primers 27 F (5'-AGAGTTT-GATCMTGGCTCAG-3') and 1492 R (5'-TACGGYTACCTTGTACGACTT-3'). We opted for full-length 16S rRNA gene sequencing to identify the relative abundance of microorganisms within the mixed microbial community. The PCR-amplified samples, indexed with specific primers,

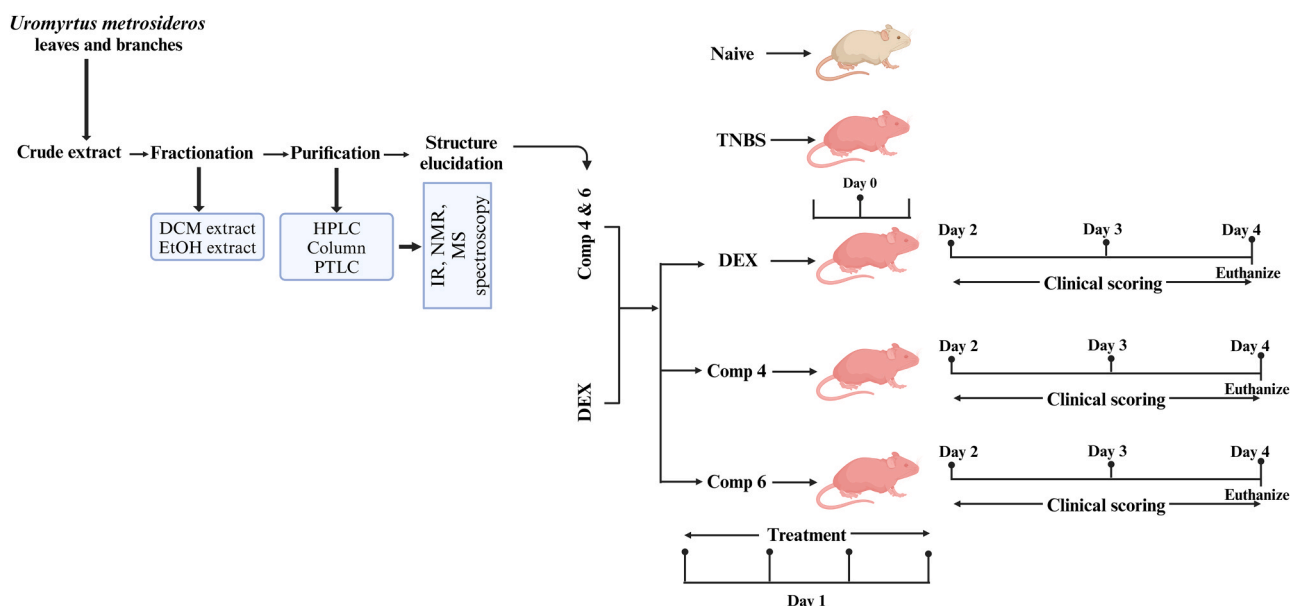


Fig. 1. Schematic overview of the plant compound extraction process and subsequent animal study. Colitis was induced in mice using TNBS, followed by selective treatments with comp-4, comp-6 and DEX.

were pooled, and sequenced using PacBio's SMRT Bell sequencing technology through AGRF in Brisbane. A total of 25 biological samples ($n = 5$ per group) were initially submitted for sequencing; however, four samples failed to amplify during PCR at AGRF. Though the microbiome analysis included fewer samples due to sequencing company QC failure, the results were consistent and reproducible across biological replicates, supporting the observed treatment effects. Thus, 21 samples were successfully sequenced and included in downstream analyses: Naïve ($n = 4$), TNBS ($n = 5$), DEX ($n = 5$), Comp-4 ($n = 3$), and Comp-6 ($n = 4$). Each successful DNA sample was amplified in triplicate PCR reactions to minimize amplification bias, and technical replicates were pooled prior to library preparation.

2.3. Microbiome sequence data analysis

PacBio HiFi full-length 16S data was quality-filtered and "denoised" into high-quality amplicon sequence variants (ASVs) using QIIME2 and DADA2. ASV classification was performed using two approaches. First, we conducted a consensus alignment classification using VSEARCH against the Genome Taxonomy Database (GTDB r207) (Parks et al., 2022), ensuring high consistency in taxonomic assignment. In addition, we employed a naive Bayesian machine learning classification approach (DADA2) (Callahan et al., 2016; Parks et al., 2022), using a three-tiered database system that successively searches the next database if a species-level match is not found. The databases used, in order, were the Genome Taxonomy Database (GTDB r207) (Parks et al., 2022), the SILVA rRNA database (v138) (Quast et al., 2012), and the NCBI RefSeq 16S rRNA database (O'Leary et al., 2016), supplemented by the Ribosomal Database Project (RDP) (Cole et al., 2014). This method allows for better classification of low-abundance ASVs. Microbial diversity within the samples (α diversity) was assessed using the Observed, Shannon, and Simpson indices, while β diversity was evaluated through an unweighted UniFrac distance matrix. Principal Component Analysis (PCA) based on the Bray-Curtis ordination was conducted using the R package Phyloseq V1.48 (McMurdie and Holmes, 2013). Relative abundance was calculated by normalizing raw ASV counts within each sample, dividing each count by the total number of reads to account for differences in sequencing depth. Taxa were subsequently aggregated at the phylum levels using the taxonomic agglomeration function from the phyloseq package (v1.48.0) (McMurdie and Holmes, 2013), and the top 20 most

abundant taxa were visualized based on their cumulative relative abundance across all samples. Differential abundance analysis was conducted using the R package DESeq2 v1.44 (Love et al., 2014). Given the small sample size and compositional nature of microbiome data, DESeq2 results should be interpreted with caution. All other visualizations were created with the R packages ggplot2 v3.5.1 (Wickham and Wickham, 2016) and pheatmap v1.0.12 (Kolde, 2019). Statistical analyses were performed using base R in R core. Further, the Phylogenetic Investigation of Communities by Reconstruction of Unobserved States (PICRUST2) (Douglas et al., 2020) was utilized to predict the functions of the gut bacterial community through the MetaCyc database.

2.4. In-silico structural analysis and molecular dynamics (MD) simulations

Based on our previous findings, the chemical structures of comps 4 and 6 were meticulously constructed using ChemDraw Pro v21.0.0 (PerkinElmer Informatics, Inc.) (Jabi et al., 2024) and generated SMILES using SwissTargetPrediction (<http://www.swisstargetprediction.ch/>) server (Daina et al., 2019). Three-dimensional (3D) structures of the ligands were generated using Chem3D Pro v21.0 (PerkinElmer Informatics, Inc.) with Allinger's force field (MM_2) employed for energy minimization (Bappi et al., 2024). The resultant molecular models were then imported into LigandScout v4.5, a sophisticated software platform designed for pharmacophore modelling and physicochemical properties analysis (Wolber and Langer, 2005). The human protein structure (IL-6, IL-8, IL-10, IL-17A, IFN- γ , and TGF- β_{1-3}) was obtained from the UniProt database (<https://www.uniprot.org/>), and the most validated protein model was selected from AlphaFold, a cutting-edge AI-based platform known for its high-confidence predictions of protein folds (Jumper et al., 2021). The structure was further refined using Swiss-PDB Viewer v4.1.0, with energy minimization performed using the GROMOS 96 43B1 force field, ensuring structural accuracy for docking studies. Docking simulations were performed with CB-Dock2 (<https://cadd.labshare.cn/cb-dock2/>), an advanced AI-driven blind docking tool, to predict the most likely binding sites and optimal binding poses of the ligands to the protein (Liu et al., 2022). The protein-ligand complex was visualized and analysed using PyMOL v3.0 (Schrödinger), providing detailed structural insights into the ligand binding interactions (DeLano, 2002). The docking stability was further assessed by conducting molecular

dynamics (MD) simulations using Schrödinger Release 2020–4 (Academic) along with Desmond v6.4. All simulations were carried out on a Linux (Ubuntu 22.04.4 LTS) system with an Intel® Xeon® Gold 6430 processor and NVIDIA GA102GL [RTX A6000] GPUs. To prepare the system for MD simulations, it was neutralized with Na⁺ and Cl[−] ions, and the OPLS-2005 force field was applied for the protein-ligand system (Shivanika et al., 2020). The simulations were conducted for a duration of 100 ns under NPT conditions, maintaining a constant temperature of 300 K and pressure of 1.01325 bar. The stability of the protein-ligand complex was assessed using several metrics, including trajectory performance, root mean square fluctuation (RMSF), root mean square deviation (RMSD), solvent-accessible surface area (SASA), intramolecular hydrogen bonds (intraHBs), radius of gyration (Rg), protein-ligand contacts (PL), polar surface area (PSA), and molecular surface area (MolSA) (Islam et al., 2024).

2.5. Statistical analysis

Statistical analyses were performed using R software (version 4.3.1) and GraphPad Prism (version 8.4.3). Data normality was assessed with the Shapiro-Wilk test. Differential abundance analysis was conducted using the DESeq2 package (v1.44.0) in R, which models count data with negative binomial generalized linear models and adjusts for multiple testing using the Benjamini-Hochberg false discovery rate (FDR) correction. Alpha diversity indices (Observed, Shannon, Simpson) were compared across groups using the non-parametric Kruskal-Wallis test with Dunn's post hoc test for pairwise comparisons. Beta diversity differences were assessed by permutational multivariate analysis of variance (PERMANOVA) on Bray-Curtis dissimilarity matrices using the vegan package (v2.6–4). Additional statistical tests and graphical visualizations were performed in GraphPad Prism. Statistical significance was set at $p < 0.05$ unless otherwise specified.

3. Results

3.1. TNBS-induced colitis alleviates via novel plant compounds

To assess colitis severity and therapeutic effects of treatment, we monitored body weight changes and evaluated composite macroscopic and clinical scores across experimental groups. Following TNBS administration, mice exhibited a rapid and considerable reduction in body weight compared to naive controls, reaching the lowest point on day 2. The earlier and relatively milder weight loss observed in our study, compared to the prolonged reduction typically reported in TNBS models, likely reflects differences in strain background, dosing, and experimental conditions. This outcome highlights the moderate, yet consistent disease phenotype achieved in our study. While a partial recovery was observed by day 5, TNBS-induced mice maintained a lower body weight trajectory (Fig. 2A). Mice treated with comp-4 demonstrated more pronounced recovery, followed by DEX and comp-6 groups, suggesting a treatment-associated attenuation of weight loss. Macroscopic scoring, based on observable signs of inflammation such as colon thickening, oedema and adhesions (Figure S1A-C), was significantly elevated in the TNBS group compared to naive controls. Treatment with comp-4 led to a notable reduction in macroscopic scores, among the experimental groups, while DEX and comp-6 did not reduce inflammation compared to TNBS (Fig. 2B). Similarly, the overall clinical score, calculated from parameters including weight loss, stool consistency, rectal bleeding, and piloerection, was elevated in TNBS-induced mice, but was ameliorated to varying extents by the administered treatments (Fig. 2C & Figure S1D, E). Among the test compounds, comp-4 was most effective in reducing the clinical score, indicating its superior anti-inflammatory activity. Representative images of colon tissue further illustrate these gross pathological changes. TNBS colons displayed oedema, hyperaemia, and thickening, which were visibly ameliorated in the comp-4 and DEX groups, while comp-6 treatment led to partial improvement (Fig. 2D). It is important to note that Fig. 2D presents all five colon samples per group, and macroscopic scoring was performed in a blinded and standardised manner across all samples. This

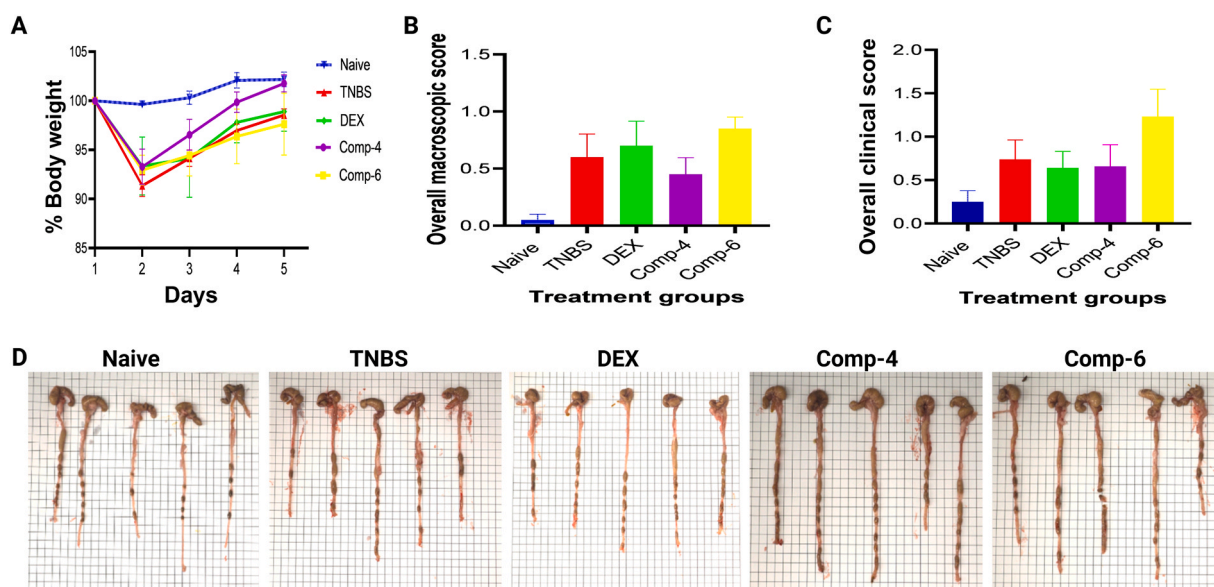


Fig. 2. Assessment of body weight, macroscopic damage, and clinical severity in TNBS-induced colitis. (A) Percentage change in body weight over five days post-induction across naive, TNBS, DEX, comp-4, and comp-6 treatment groups. TNBS-induced mice showed significant weight loss compared to naive controls, with partial recovery observed in treated groups. (B) Overall macroscopic score reflecting gross pathological changes in the colon. (C) Overall clinical score based on cumulative evaluation of disease indicators including weight loss, stool consistency, rectal bleeding, and piloerection. (D) Representative images of colon tissue illustrating gross pathological changes. TNBS-treated colons exhibited oedema, hyperaemia, and thickening, which were visibly ameliorated in the comp-4 and DEX groups, with partial improvement in comp-6. Data are presented as mean \pm SEM ($n = 5/\text{group}$, $p < 0.05$). These findings confirm disease induction and highlight the protective effects of comp-4 and comp-6 against TNBS-induced colitis.

semi-quantitative scoring, based on colon thickening, oedema, hyperaemia, and adhesions (Dieleman et al., 1998), consistently showed that comp-4 achieved slightly lower inflammation scores than DEX, even though some DEX colons appeared visually closer to naive controls. This difference reflects the greater sensitivity of numerical scoring which captures subtle inflammatory changes in all samples that may not be apparent in representative Fig. 2D. Taken together, both comp-4 and DEX demonstrated protective effects, with comp-4 showing the strongest overall improvement across the combined parameters. These findings confirm successful model induction and demonstrate the therapeutic potential of plant-derived interventions in mitigating colitis severity.

3.2. Gut microbial diversity and taxonomic abundance

The gut microbiota diversity of mice across different groups were assessed by using 16S rRNA sequencing. Alpha diversity metrics, including the Observed, Shannon, and Simpson indices, were utilized to evaluate the microbial communities. The findings indicated that TNBS treatment significantly reduced the observed richness, while the Shannon and Simpson indices showed a notable increase when compared to the naive group. In contrast, the Shannon and Simpson indices for the comp-4, comp-6, and DEX (standard drug control) groups were almost similar to those of the TNBS group but were significantly higher than

those of the Naive group. Additionally, the observed richness for comp-4, comp-6, and DEX groups was markedly greater than that of the TNBS group (Fig. 3A). A Principal Component Analysis (PCoA), which serves as a beta diversity analysis, revealed distinct structural shifts in the gut microbiota among the five groups (Fig. 3B). Overall, the results demonstrated that the community richness of the gut microbiota varied across the five experimental groups.

As illustrated in Fig. 3C, the phyla *Bacteroidota* and *Firmicutes* emerged as the most prevalent gut microbiota among the five experimental groups. Other phyla identified included *Proteobacteria*, *Desulfobacterota*, *Cyanobacteria*, *Verrucomicrobiota*, *Actinobacteriota* and *Campylobacterota*. Notably, TNBS treatment led to an increase in the relative abundances of *Proteobacteria* and *Bacteroidota*, as well as *Verrucomicrobiota* while concurrently resulting in a decrease in the relative abundance of *Firmicutes* when compared to the naive group at the phylum level. Further taxonomic profiling at the order, family, and genus levels demonstrated a TNBS-induced dysbiosis characterised by alterations in key microbial taxa. Treatment with the test compounds partially restored a symbiotic microbial composition. Notable taxa involved in this shift included *Bacteroidales* (order), *Lachnospirales* (order), *Bacteroidaceae* (family), and *Lactobacillus* (genus) etc. (Figure S2A-C). Consistent with these findings, treatment with comps 4, 6, and DEX promotes reshaping of the microbial community and helps maintain homeostatic conditions within the gut.

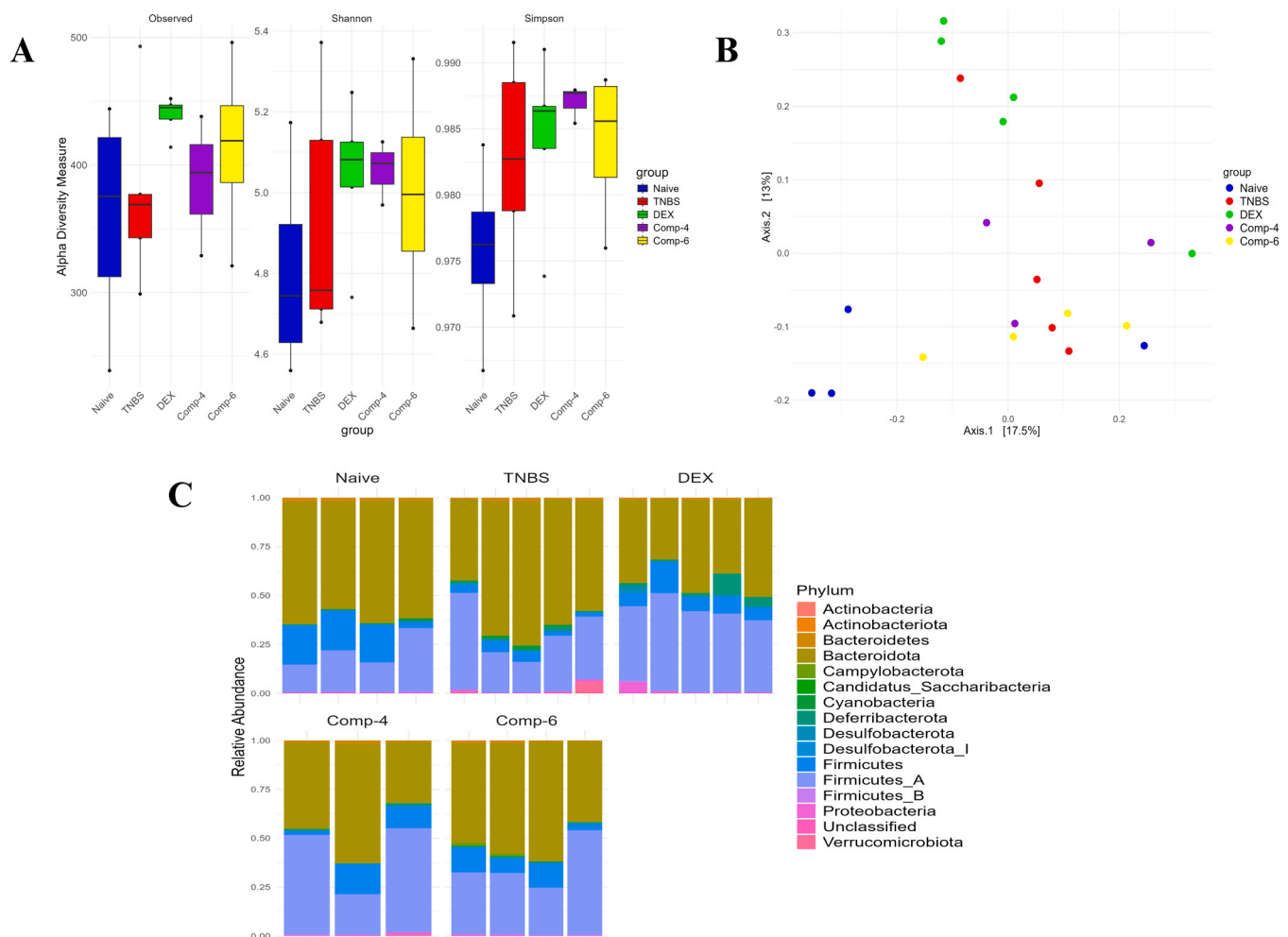


Fig. 3. Gut microbial diversity and community composition in the TNBS-induced colitis mouse model. (A) Alpha diversity, represented by Observed species, Shannon, and Simpson indices, was used to assess microbial diversity within samples. (B) Beta diversity was visualized using Principal Component Analysis (PCoA) plots based on Bray-Curtis ordination, highlighting differences between operational taxonomic units (OTUs) across groups. (C) Relative abundance plots were generated to display variations in microbial community structure at the phylum level, focusing on the top 20 most abundant taxa.

3.3. Plant compounds restore imbalanced gut microbial species

At species level (Fig. 4), we identified four bacterial species of interest within the phylum *Firmicutes*: *S. ureilyticus*, *A. muris* A, *M. pectinilyticus*, and *S. pneumoniae*. Among these, *S. ureilyticus* species was abundant in naïve mice but showed a significant decrease in the abundance in TNBS-induced colitis mice (*S. ureilyticus*: -17.38 log₂ fold change, $p = 4.40\text{E-}43$). Notably, TNBS-induced colitis mice treated with comps 4, 6, and DEX resulted in restoring dysbiotic bacterial species including a significant increase of the abundance of *S. ureilyticus* (16.38 log₂ fold change, $p = 1.78\text{E-}32$ for comp-4; 14.58 log₂ fold change, $p = 3.94\text{E-}8$ for comp-6; 26.47 log₂ fold change, $p = 9.78\text{E-}21$ for DEX).

In contrast, the remaining three *Firmicutes* species exhibited significantly higher in abundances in TNBS-induced colitis mice compared to naïve mice (*A. muris* A: 11.59 log₂ fold change, $p = 9.59\text{E-}6$; *M. pectinilyticus*: 24.45 log₂ fold change, $p = 3.47\text{E-}14$; *S. pneumoniae*: 23.15 log₂ fold change, $p = 7.23\text{E-}13$). Interestingly, treatment with these compounds led to a significant decrease in the abundance of

A. muris A (-11.39 log₂ fold change, $p = 3.02\text{E-}05$ for comp-4; -11.41 log₂ fold change, $p = 5.38\text{E-}07$ for DEX), *M. pectinilyticus* (-23.59 log₂ fold change, $p = 2.45\text{E-}11$ for comp-4; -23.66 log₂ fold change, $p = 2.16\text{E-}13$ for comp-6; -24.54 log₂ fold change, $p = 5.06\text{E-}16$ for DEX) and *S. pneumoniae* (-22.66 log₂ fold change, $p = 1.45\text{E-}10$ for comp-4; -23.17 log₂ fold change, $p = 6.87\text{E-}13$ for comp-6).

Within the phylum *Bacteroidetes*, we observed a significant increase in the abundances of *P. merdae* in the TNBS-induced colitis group (22.84 log₂ fold change, $p = 1.46\text{E-}12$). However, TNBS-induced colitis mice treated with comp-6 and DEX led to a significant reduction in the abundance of *P. merdae* (-23.90 log₂ fold change, $p = 1.27\text{E-}13$ for comp-6; -24.05 log₂ fold change, $p = 1.91\text{E-}15$ for DEX).

Furthermore, we observed a significant increase in the abundance of *H. influenzae* from the phylum *Proteobacteria*, in the TNBS-induced colitis group (23.46 log₂ fold change, $p = 3.59\text{E-}13$). Remarkably, TNBS-induced colitis mice treated with comps 4 and 6 resulted in a sharp reduction (-22.84 log₂ fold change, $p = 1.03\text{E-}10$ for comp-4; -23.52 log₂ fold change, $p = 3.10\text{E-}13$ for comp-6) of this species.

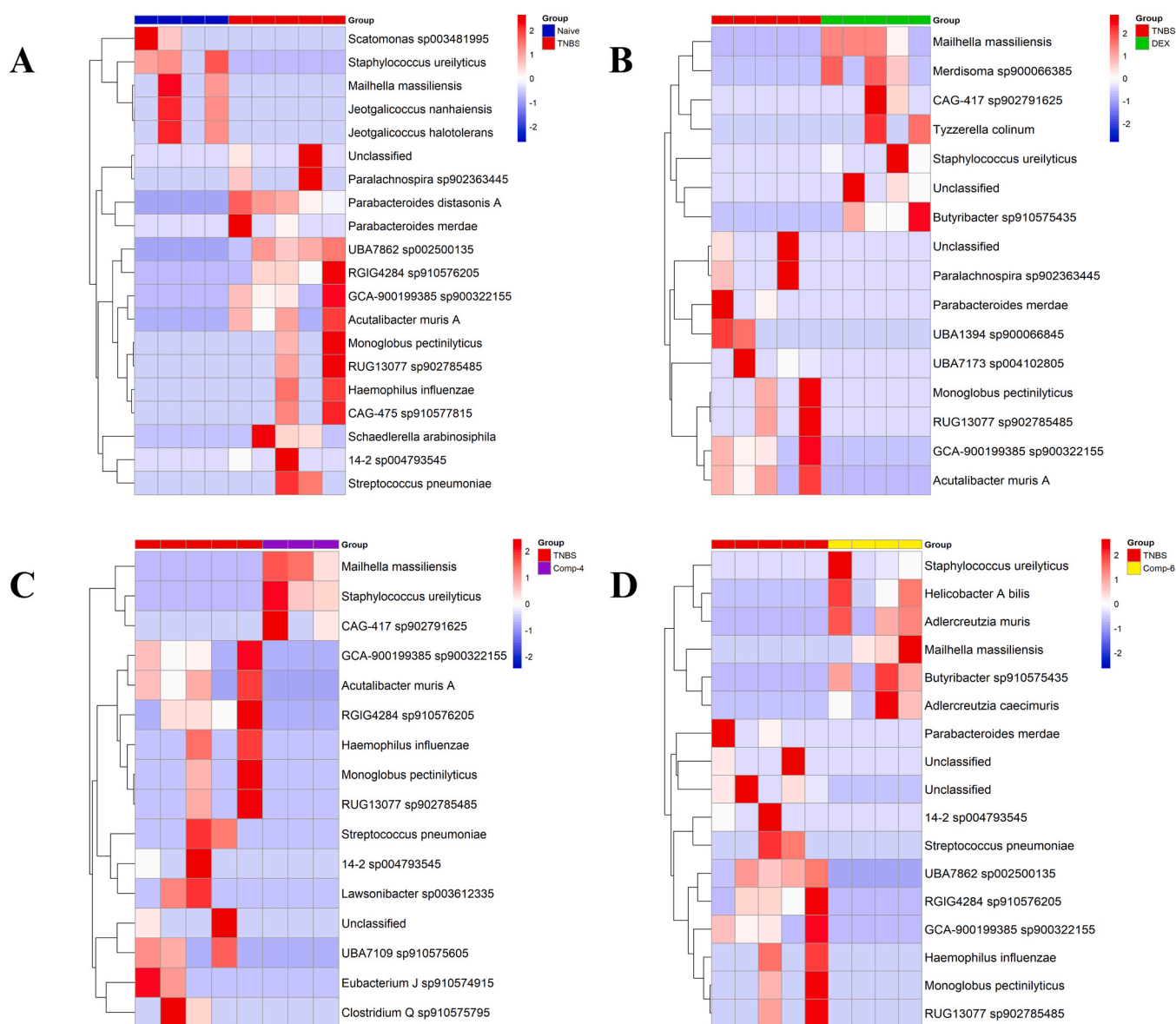


Fig. 4. Species level gut microbial diversity in the TNBS-induced colitis mouse model. Heatmaps depicting the relative abundance of the top 20 bacterial species across experimental groups. Comparisons include (A) Naive vs. TNBS, (B) TNBS vs. DEX, (C) TNBS vs. comp-4, and (D) TNBS vs. comp-6. These heatmaps reveal distinct alterations in microbial composition associated with each treatment condition, emphasizing differences in bacterial community structure between groups (please see Figure S3 for further details).

Finally, we identified a lower-abundance bacterium, *M. massiliensis*, within the phylum *Desulfobacterota*, which were significantly reduced levels in TNBS-induced colitis mice compared to naïve group of mice ($-24.95 \log_2$ fold change, $p = 5.64E-15$). Significantly, TNBS-induced colitis mice treated with comps 4, 6, or DEX led to a substantial increase in the abundance of *M. massiliensis* ($11.51 \log_2$ fold change, $p = 2.75E-05$ for comp-4; $10.11 \log_2$ fold change, $p = 0.00044$ for comp-6; $10.74 \log_2$ fold change, $p = 3.63E-06$ for DEX).

3.4. Functional effects of gut microbiome associated with comps 4, 6 and DEX

Understanding taxonomic shifts in the gut microbiota is crucial, but it is equally important to assess the functional consequences of these changes to fully identify their broader implications. To this end, we employed full-length 16S rRNA gene sequencing in combination with PICRUST2 to predict the functional pathways. As shown in Fig. 5, several metabolic pathways were significantly altered following treatment with plant-derived compounds and DEX, with only those pathways that exhibited notable changes related to our plant-compound being presented in Fig. 6. STAMP analysis also revealed a total of 56 altered pathways when comparing the naïve and TNBS-treated groups. Notably, treatment with comp-4 resulted in only 7 altered pathways, while treatment with comp-6 led to 8 altered pathways. On the other hand, treatment with the standard DEX regimen caused a significant increase in the number of altered pathways, reaching 17. These findings highlight distinct and significant functional shifts in the gut microbiota following treatment with plant-derived compounds, suggesting that these treatments may have profound effects on the gut's metabolic processes and microbiome composition.

The administration of plant-derived compounds (comps 4, 6) and

standard drug (DEX) led to significant alterations in various gut microbial metabolic pathways. Notably, in TNBS-induced colitis mice, populations of gut microbes involved in the peptidoglycan biosynthesis pathways II, IV, and V (Fig. 6A-C) were markedly reduced compared to the control group. However, treatment with comps 4 and 6 significantly increased the abundance of microbial populations associated with peptidoglycan biosynthesis pathway IV. Comp-4 also increased the populations linked to peptidoglycan biosynthesis pathways II and V, while DEX and comp-6 had a lesser effect. This aligns with findings by Lo Sasso et al. (2021), who reported that an overabundance of peptidoglycan biosynthesis often associated with an increased abundance of *Lactobacillaceae* (Lo Sasso et al., 2021). In line with these findings, Matsumoto et al. (2009) demonstrated that *Lactobacillus casei* Shirota and its cell wall-derived polysaccharide-peptidoglycan complex (PSPG) can inhibit IL-6 production (Matsumoto et al., 2009).

Additionally, TNBS-induced colitis mice exhibited a significant increase in microbial populations related to L-tryptophan biosynthesis (Fig. 6D) compared to the control group. Interestingly, comps 4, 6, and DEX significantly reduced these populations. Tryptophan, an essential amino acid, is metabolized through several pathways in the gut, including the kynurenine pathway, which is closely linked to inflammation. These findings are consistent with previous studies in mice, where overactivation of the kynurenine pathway was associated with increased inflammatory responses (Michaudel et al., 2023).

Furthermore, TNBS-induced colitis mice showed a notable decrease in microbial populations associated with the Bifidobacterium shunt pathway (Fig. 6E) compared to the control group. However, treatments with comps 4, 6, and DEX significantly increased these populations. The Bifidobacterium shunt, or fructose-6-phosphate shunt, is a unique carbohydrate metabolism pathway that is critical for the survival and proliferation of Bifidobacteria (Devika and Raman, 2019). This pathway

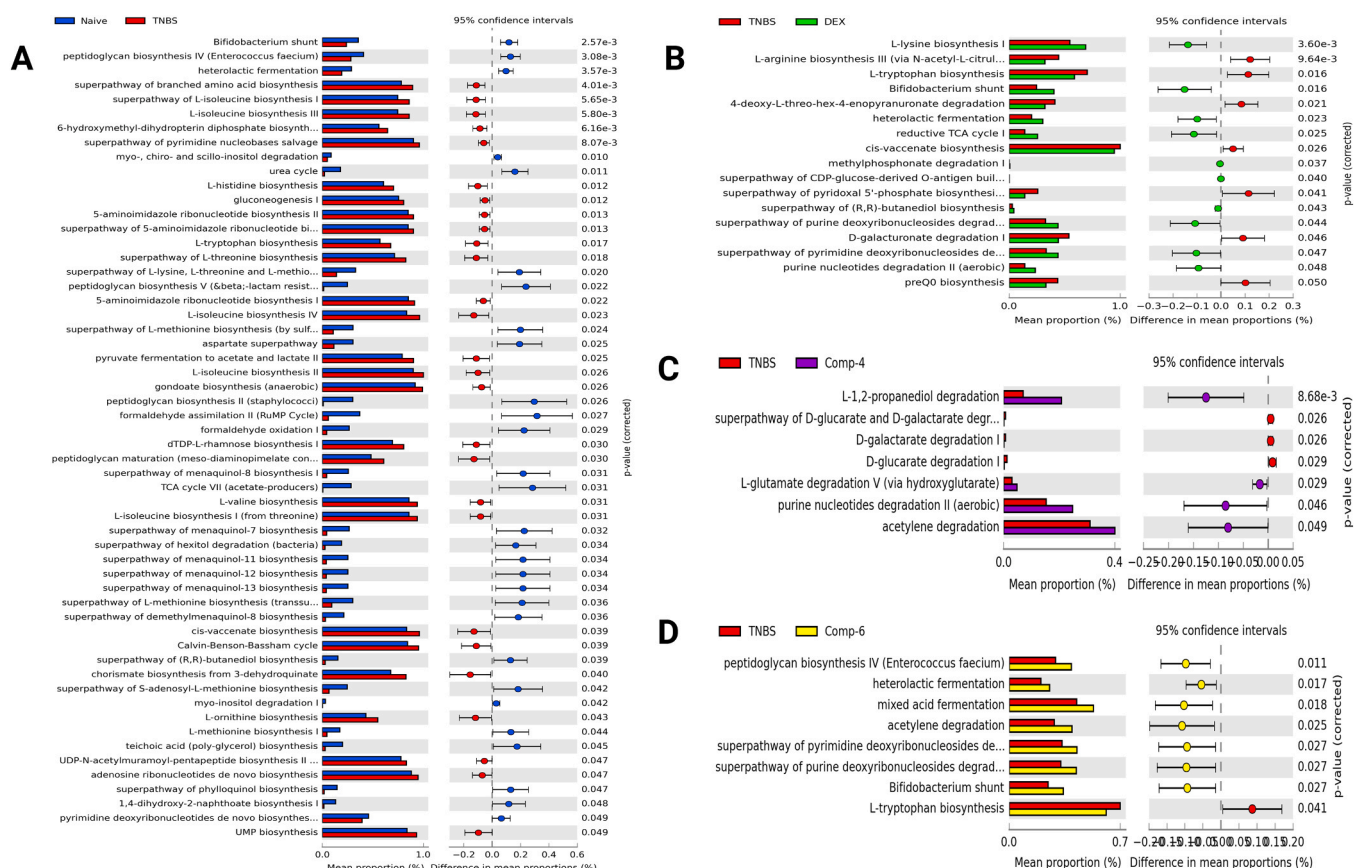


Fig. 5. Function prediction of the gut microbiota revealed using PICRUST2. Naive vs. TNBS (A), TNBS vs DEX (B), TNBS vs Comp-4 (C), TNBS vs Comp-6 (D) ($p < 0.05$, confidence intervals = 95 %).

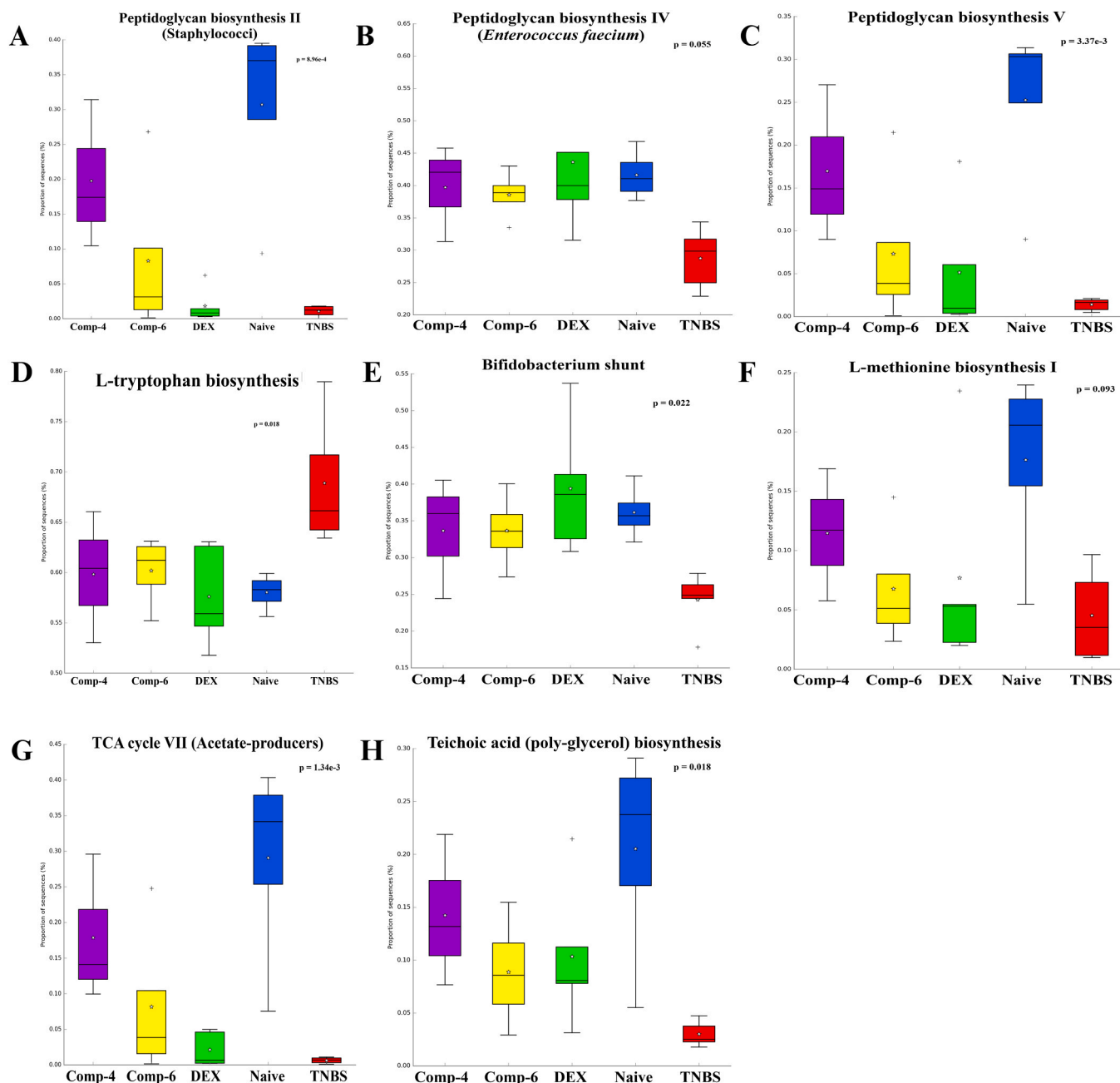


Fig. 6. Predicted individual functional composition of the gut microbiome. Functional profiles were inferred using metagenomic prediction tools, with statistical differences assessed by one-way ANOVA followed by the Tukey-Kramer post hoc test for multiple comparisons ($p < 0.05$) in STAMP (version v2.1.3). Box plots denote the top quartile, median, and bottom quartile, and white stars mean the average value. The analysis identifies significant shifts in microbial functional pathways, offering insights into the metabolic and physiological changes associated with each experimental condition (Please see [Figure S4](#) for details pathways).

contributes to the production of short-chain fatty acids (SCFAs) such as acetate and lactate, which play essential roles in gut health and epithelial barrier integrity ([Abdulqadir et al., 2023](#)). Moreover, TNBS-induced colitis mice treated with comps 4, 6, and DEX exhibited significant increase in microbial populations involved in other key metabolic pathways, including L-methionine biosynthesis I ([Fig. 6F](#)), TCA cycle VII (acetate-producing pathways) ([Fig. 6G](#)), and poly-glycerol teichoic acid biosynthesis ([Fig. 6H](#)).

3.5. Structural analysis and molecular docking of cytokine interactions with comps 4 and 6

The pharmacophore and physicochemical properties analysis

revealed that comp-4 [canonical SMILES: CC(=O)CCC1=C(O[C@@H]2O[C@H](COC(=O)C3=CC(O)=C(O)C(O)=C3)[C@@H](O)[C@H](O)[C@H]2O)C(C)=C(O)C(C)=C1O; chemical formula: $C_{25}H_{30}O_{13}$; molecular weight: 537.16 g/mol; topological polar surface area (TPSA): 223.67 \AA^2 ; molar refractivity: 129.86; water solubility, ESOL (Log S): -3.01 (soluble)] contains 12 hydrogen bond acceptors (HBA) and 8 hydrogen bond donors (HBD) ([Fig. 7A, B](#)), whereas comp-6 [canonical SMILES: CCCCC1C(O)C(C)C(O)C(C)(C)C1O[C@@H]1O[C@H](COC(=O)C2=CC(O)=C(O)C(O)=C2)[C@@H](O)[C@H](O)[C@H]1O; chemical formula: $C_{26}H_{40}O_{12}$; molecular weight: 543.24 g/mol; topological polar surface area (TPSA): 206.60 \AA^2 ; molar refractivity: 133.81; water solubility, ESOL (Log S): -3.61 (soluble)] contains 11 HBAs and 8 hydrogen HBDs. Hydrogen bonds are key to the binding affinity and

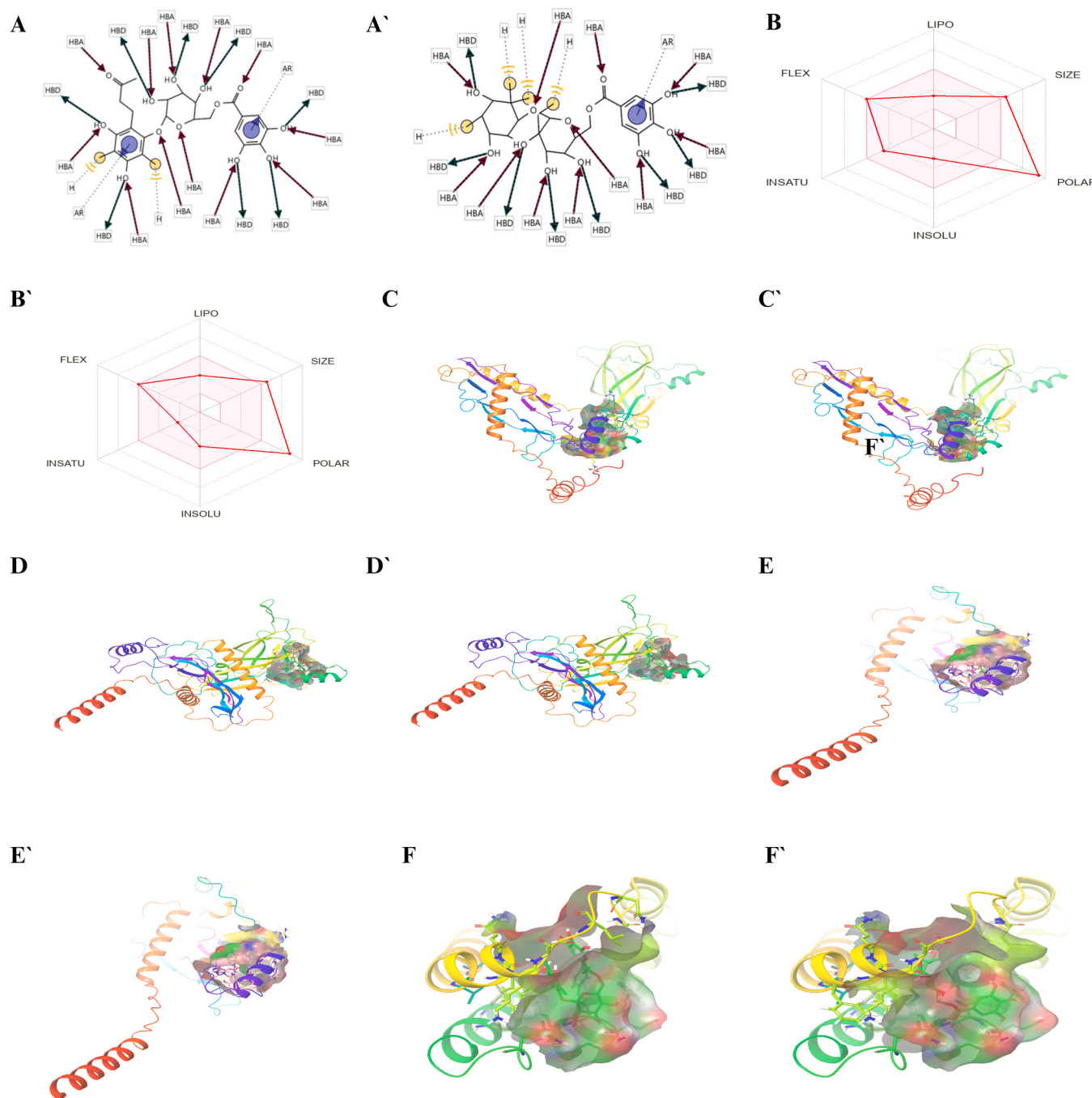


Fig. 7. Pharmacophore structure analysis was performed for Comp-4(A) and Comp-6(A'), along with ADME predictions for Comp-4(B) and Comp-6(B'). Molecular docking results highlight the interactions of Comp-4 and Comp-6 with core targets, (C) Comp-4 + TGFβ1, (C') Comp-6 + TGFβ1, (D) Comp-4 + TGFβ2, (D') Comp-6 + TGFβ2, (E) Comp-4 + TGFβ3, (E') Comp-6 + TGFβ3, (F) Comp-4 + IL-10, and (F') Comp-6 + IL-10.

specificity of a molecule to its target protein (Fig. 7 A', B'). A higher number of HBAs and HBDs in a compound suggests it has the potential to form more stable and specific interactions with the protein, potentially enhancing its biological activity or therapeutic effect.

Molecular docking study showed that comp-4 exhibits very strong binding affinity to anti-inflammatory cytokines, TGF-β₁ (-7.6 kcal/mol) (Fig. 7C), TGF-β₂ (-8.8 kcal/mol) (Fig. 7D), TGF-β₃ (-8.4 kcal/mol) (Fig. 7E), and IL-10 (-7.6 kcal/mol) (Fig. 7F), which may enhance the anti-inflammatory activity. In contrast IFN-γ (-7.1 kcal/mol), IL-6 (-6.9 kcal/mol), IL-8 (-6.8 kcal/mol), and IL-17A (-6.6 kcal/mol) also shows significant affinity with comp-4 (Figure S5), which may play a role in the inhibitory action by reacting with cytokines. In addition,

comp-6 exhibits good affinity to anti-inflammatory TGF-β₁ (-7.7 kcal/mol) (Fig. 7C'), TGF-β₂ (-8.3 kcal/mol) (Fig. 7D'), TGF-β₃ (-8.4 kcal/mol) (Fig. 7E'), and IL-10 (-7.3 kcal/mol) (Fig. 7F') and inflammatory cytokines IFN-γ (-7.2 kcal/mol), IL-6 (-7.1 kcal/mol), IL-17A (-6.8 kcal/mol), and IL-8 (-5.6 kcal/mol) (Figure S5).

3.6. Molecular dynamics simulation of IL-10 and TGF-β receptors with lead compounds 4 and 6

A molecular dynamics (MD) simulation study was conducted to evaluate the stability of IL-10, TGF-β₁, TGF-β₂, and TGF-β₃ receptor interactions with lead comps 4 and 6, identified through molecular

docking and hydrogen bond interaction analysis. Using Desmond v3.6, 100-ns, simulations were performed for both compounds, and their stability and binding characteristics were assessed through root mean square deviation (RMSD) and root mean square fluctuation (RMSF) analyses. Complex models of the receptor-ligand interactions were generated by superimposing the targeted proteins. RMSD plots for the protein-ligand complexes over the 100-ns simulation period demonstrated consistent stability of the interactions (Figure S6). Additionally, RMSF analysis provided detailed insights into the flexibility of both the proteins and ligands during the simulations, further supporting the robust binding of these compounds (Figure S6). These results indicate that comps 4 and 6 exhibit strong and stable binding affinities to anti-inflammatory cytokines, particularly TGF- β 2, TGF- β 3, and IL-10.

4. Discussion

IBD is a chronic and recurrent gastrointestinal disorder with global prevalence. While the exact aetiology of IBD remains unclear, evidence suggests that it arises from a complex interplay between environmental factors, genetic predisposition, host susceptibility, immune dysregulation, and gut microbiota (Adolph et al., 2022; Rahaman et al., 2025). Due to lack of this clear understanding and the effective cure for IBD, many patients are using herbal medicines and few plant-derived molecules have emerged as promising therapeutic agents for IBD due to their unique structures, minimal adverse effects, and favourable outcomes in experimental models (Chen et al., 2019; Chen et al., 2021; Gong et al., 2022). To confirm the reliability of the TNBS-induced colitis model used in this study, we first validated disease induction using established clinical and macroscopic parameters. TNBS-treated mice exhibited significant weight loss, increased macroscopic damage, and elevated clinical scores compared to naive controls, confirming successful colitis induction and providing a robust foundation for therapeutic evaluation.

Over the past decade, there has been significant interest in the potential role of gut microbiota in maintaining the structure and functionality of the gastrointestinal tract (Wu et al., 2021). Dysregulated gut microbiota—characterised by altered microbial composition and diversity—is commonly observed in IBD patients and experimental models, where it contributes significantly to disease pathogenesis. As such, therapeutic strategies targeting gut microbiota modulation are increasingly explored (Cohen et al., 2019; Caenepeel et al., 2020). This study investigated the effects of comps 4 and 6 on gut microbiota in a TNBS-induced colitis mouse model, revealing significant alterations in microbial diversity and structure. Notably, TNBS treatment disrupted microbial community richness and composition, as evidenced by Shannon, Simpson, and PCoA indices. Treatments with comps 4 and 6 modulated these disruptions, demonstrating therapeutic potential.

The gut microbiota of TNBS-induced mice was dominated by the phyla *Bacteroidota* and *Firmicutes*, whose relative abundances are closely linked to intestinal health (Grigor'eva, 2020; Rahaman et al., 2025). At lower taxonomic ranks, specific species such as *S. ureilyticus* (*Firmicutes*), *P. merdae* (*Bacteroidota*), and *H. influenzae* (*Proteobacteria*) were significantly altered following TNBS induction, consistent with microbial shifts seen in IBD. Treatment with comps 4 and 6 modulated these species-level disruptions, suggesting therapeutic rebalancing. Other phyla, including *Campylobacteriia*, *Patescibacteriia*, *Actinobacteriota*, and *Desulfobacterota* (*M. massiliensis*), were also identified, consistent with previous studies (Jia et al., 2024). *Firmicutes* to *Bacteroidota* (F/B) ratio, a marker associated with colitis severity (Guo and Li, 2019; Peng et al., 2019), was reshaped by treatments with comps 4 and 6, which decreased the abundances of *Bacteroidota*, *Firmicutes*, and *Proteobacteria*. Consistent with our findings, certain species within the phyla *Firmicutes* and *Desulfobacterota*—including *M. massiliensis* showed increased abundance following treatment, suggesting a shift microbial symbiosis.

Dysbiosis observed in TNBS-treated mice included altered abundances of specific bacterial species. Treatment with comp-4 and comp-6 restored many of these species to a symbiotic state, which was

comparable to that of the standard drug, DEX. For example, *S. ureilyticus* and *M. massiliensis* were reduced in the TNBS group but were restored following treatment. Similarly, elevated levels of *A. muris*, *A. pectinilyticus*, *S. pneumoniae*, *P. merdae*, and *H. influenzae* in the TNBS group were normalized through selective treatments. These findings underscore the ability of plant-derived compounds to re-establish microbial homeostasis.

Building on these microbial shifts, this study also highlights the therapeutic potential of plant-derived compounds in modulating gut microbial functions (Figs. 5, 6) and provides valuable insights into the metabolic disruptions associated with TNBS-induced colitis. Peptidoglycan fragments derived from the human gut microbiota play a crucial role in maintaining the symbiotic relationship by supporting immune system regulation and promoting microbial balance within the intestinal environment (Berkel, 2023). Our study indicates that TNBS induction led to a reduction in the pathways of peptidoglycan biosynthesis II, IV, and V pathway while treatment with comps 4 and 6 helps to increase the peptidoglycan biosynthesis pathway, with comp-4 exhibiting greater efficacy. Peptidoglycan biosynthesis is closely linked to the presence of *Lactobacillaceae*, which supports gut health by inhibiting pro-inflammatory cytokines like IL-6 (Lo Sasso et al., 2021). *Lactobacillus casei* Shirota and the cell wall-derived polysaccharide-peptidoglycan complex (PSPG) has been shown to inhibit IL-6 production, a key cytokine responsible for inflammation in the gut (Atreya and Neurath, 2005; Matsumoto et al., 2009). These observations further emphasize the link between peptidoglycan biosynthesis and gut health.

Furthermore, L-tryptophan, an essential amino acid obtained through the diet, plays a pivotal role in regulating gut microbiota through its metabolism (Taleb, 2019). In a TNBS-induced colitis mouse model, we observed a marked increase in L-tryptophan biosynthesis. Notably, our findings demonstrate that treatments incorporating comps 4 and 6 significantly reduced L-tryptophan biosynthesis, underscoring their broader influence on gut microbial dynamics and activity. This reduction suggests a modulation of pathways linked to the pathogenesis of IBD, particularly the kynurenine pathway of tryptophan metabolism, which is well-known for its association with inflammation (Michaudel et al., 2023). These results suggest a promising mechanism through which plant-derived treatments can reduce inflammatory pathways and support a healthier gut environment.

In parallel, the modulation of other critical microbial pathways, such as the Bifidobacterium shunt pathway, which generates short-chain fatty acids, including butyrate and acetate that plays a crucial role in maintaining intestinal homeostasis, providing energy for epithelial cells, and enhancing gut barrier integrity (Sela et al., 2008; Parada Venegas et al., 2019). Our results demonstrate that TNBS-induced mice showed a significant reduction of Bifidobacterium shunt pathway, while mice treated with comps 4 and 6 found to be promising candidate in increasing the functional activity of this pathway. Previous study indicate carbohydrate metabolism in *Bifidobacterium* follows the Bifidobacterium shunt, or fructose-6-phosphate shunt, which involves the conversion of fructose-6-phosphate from glucose to erythrose-4-phosphate via the enzyme fructose-6-phosphate phosphoketolase (Gavini et al., 1996; Pokusaeva et al., 2011; Pyclik et al., 2020). This pathway is essential for the survival and proliferation of *Bifidobacteriia*, as evidenced by knockout studies (Devika and Raman, 2019). The products of this pathway, namely acetate and lactate, are short-chain fatty acids that have beneficial effects on gut health (Abdulqadir et al., 2023). In particular, acetate contributes to increased mucus production in the intestinal barrier, which acts as both a lubricant and a physical barrier against microorganisms, toxins, and acidity resulting from digestion (Caetano and Castellucci, 2022). In addition to these metabolic shifts, *Bifidobacterium* has been shown to play a crucial role in maintaining intestinal epithelial barrier integrity and promote gut health (Fukuda et al., 2011; Bergmann et al., 2013). These findings emphasize how metabolic modulation by plant-derived compounds can restore critical microbial pathways,

offering a robust defence against gut inflammation.

While our study utilised full-length 16S rRNA gene sequencing coupled with PICRUSt2 to predict microbial functional pathways, we acknowledge the limitations inherent to amplicon-based functional inference. PICRUSt2 provides computational predictions based on phylogenetic placement, and although it has been widely used and benchmarked against shotgun metagenomic data for identifying broad functional trends, it cannot capture the full functional complexity or novel genes present in the microbiome (Langille et al., 2013; Douglas et al., 2020; Machado et al., 2024). Therefore, the predicted metabolic shifts presented here, including alterations in peptidoglycan biosynthesis, tryptophan metabolism, and Bifidobacterium shunt pathway, should be interpreted as hypothesis-generating rather than conclusive. Future studies incorporating shotgun metagenomic or metatranscriptomic sequencing will be essential to validate and expand upon these findings, offering a more comprehensive view of the microbial functional landscape in IBD.

Building on previous in-vitro study, comp-4 exhibited significant anti-inflammatory activity, notably suppressing the release of IFN- γ , IL-17A, and IL-8 in phorbol myristate acetate/ionomycin (P/I) - and anti-CD3/anti-CD28-activated immune cells. However, no significant effect was recorded on TNF release. Additionally, comp-6 notably suppressed IFN- γ secretion but did not produce significant effects on other cytokines using in-vitro assays (Ritmejeriyé et al., 2022). Further *in-silico* analysis conducted in this study, revealed that comps 4 and 6 exhibited higher binding affinities for IFN- γ , IL-17A, and IL-8, supporting their potential anti-inflammatory activity. To expand on these findings, we extended our *in-silico* evaluation to include the proinflammatory cytokine IL-6 and anti-inflammatory cytokines TGF- β 1, TGF- β 2, TGF- β 3, and IL-10. As IBD is a chronic disorder driven by excessive immune responses to intestinal flora (Zhang et al., 2017), cytokines such as TGF- β and IL-10 play critical roles in immune regulation and suppression (Moore et al., 2001; Li et al., 2006; Wan and lavell, 2007; Li and Flavell, 2008). In contrast, IL-6 contributes significantly to inflammation and the pathogenesis of IBD (Waldner and Neurath, 2014). Our computational studies suggest that comps 4 and 6 exhibit strong binding affinities for TGF- β 1, TGF- β 2,

TGF- β 3 and IL-10, implying that these compounds may enhance the levels of these cytokines in IBD patients, thereby aiding in immune suppression. Moreover, the strong binding affinity of comps 4 and 6 with IL-6 indicates their potential to reduce the levels of this inflammatory cytokine.

We also proposed a mechanistic model that integrates evidence from our previously published *in vitro* cytokine assays, current *in silico* cytokine binding analyses, and microbiome and predicted metabolic pathway data obtained from the TNBS-induced murine model of IBD. This model highlights the critical interplay between gut microbiota, epithelial integrity, and immune responses (Fig. 8). This representation elucidates the progression from bacterial dysbiosis to immune-mediated inflammation and highlights the potential for therapeutic interventions to restore homeostasis. In this model, we used a widely utilised chemical agent (TNBS) to induce colitis, which replicates the hallmark features of IBD, including epithelial barrier disruption and bacterial dysbiosis (Torres et al., 1999; Wen et al., 2024). Dysbiosis, often characterised by an imbalance in gut microbiota composition, leads to the translocation of microbial products across the damaged epithelium into the lamina propria (Rahaman et al., 2025). This breach triggers a robust immune response mediated by effector T cells (Th1, Th2, Th17) that secrete pro-inflammatory cytokines, such as IFN- γ , TNF, IL-6, IL-8, and IL-17A (Kobayashi et al., 2008; Neurath, 2014). The failure of epithelial cells, particularly Paneth cells, to secrete antimicrobial peptides such as α -defensins further exacerbates the imbalance in gut microbial communities (Bevins and Salzman, 2011). The cumulative effect of dysbiosis and cytokine-driven inflammation perpetuates epithelial damage and overwhelms regulatory T cell activity, which typically downregulate anti-inflammatory responses through the decreased production of TGF β and IL-10 (O'garra and Vieira, 2004).

The therapeutic potential of novel plant comps 4 & 6 illustrated in the figure underscores the importance of restoring gut symbiosis and promoting epithelial healing. These interventions likely enhance α -defensin secretion, aiding in microbial regulation and epithelial barrier repair (Clevers and Bevins, 2013). Restoration of microbial symbiosis shifts the immune response from a pro-inflammatory state to an

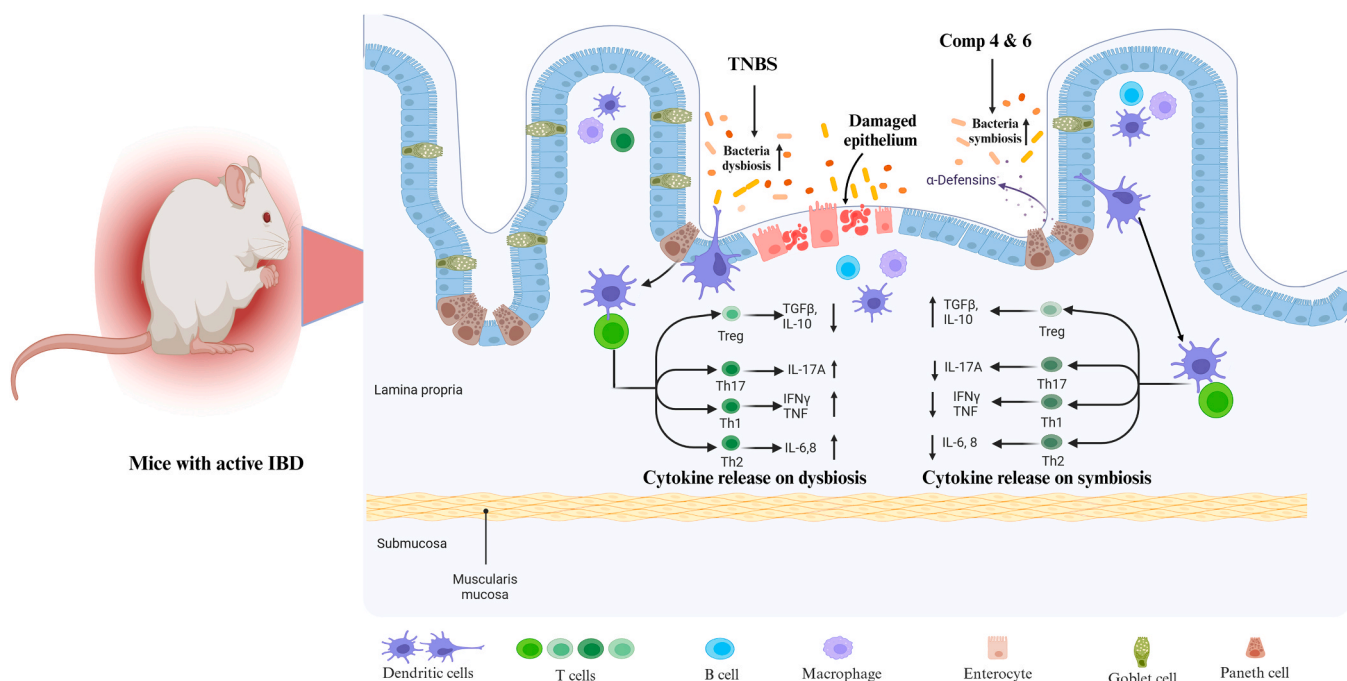


Fig. 8. Proposed mechanistic insights underlying the pathophysiology and mitigation of IBD integrates findings from *in vitro* cytokine assays, *in silico* cytokine binding analyses, and *in-vivo* microbiome study. Previous *in-vitro* and current *in-silico* data collectively suggests that the plant compounds effectively suppress pro-inflammatory cytokines (IL-6, IL-8, IL-17A, IFN- γ , and TNF) while increase anti-inflammatory mediators (TGF- β and IL-10). Consistent with these findings, *in-vivo* study indicates that TNBS-induced colitis demonstrated microbial dysbiosis. Notably, treatment with comps 4 & 6 helped to restores bacterial symbiosis.

anti-inflammatory profile dominated by Treg-mediated production of TGF β and IL-10 (Fujio et al., 2010). This rebalancing dampens the activity of effector T cells, reducing levels of IFN γ , TNF, IL-6, and IL-17A, ultimately resolving inflammation (Neurath, 2019). This murine model effectively recapitulates the complex pathophysiology of IBD, offering insights into the roles of microbial dysbiosis, in-vitro and *in-silico* study emphasise the immune dysregulation. The findings align with emerging evidence that microbiota-targeted therapies, including probiotics, prebiotics, and small molecules, hold significant promise for managing IBD (Kostic et al., 2014; Paramsothy et al., 2017). By focusing on the restoration of symbiosis and immune homeostasis, these interventions address critical drivers of disease progression.

4.1. Study limitations

Despite providing comprehensive insights into the therapeutic potential of plant-derived compounds in TNBS-induced colitis, this study has several limitations. First, the sample size for microbiome analyses was modest, particularly for the comp-4 group (n = 3), which may limit statistical power and generalisability. Second, differential abundance analysis using DESeq2, while widely used, may not fully account for the compositional nature of microbiome data. Third, functional predictions derived from PICRUSt2 are computational and may not capture the full functional repertoire of the gut microbiome. Finally, variability in TNBS-induced disease severity, influenced by strain background, dosing and experimental conditions could impact outcomes. Future studies incorporating larger cohorts, shotgun metagenomics, and experimental validation of microbial functions are essential to confirm and extend these findings.

5. Conclusions

Overall, this study reveals that treatment with comps 4 and 6 effectively modulates the gut microbiota via restoring imbalanced microbial species and enhancing beneficial functional pathways while suppressing those associated with IBD pathogenesis. Complementary *in-silico* analyses further revealed the potent anti-inflammatory and immunomodulatory properties of these compounds, reinforcing their therapeutic potential. Together, these findings underscore comps 4 and 6 as promising candidates for innovative IBD management strategies. These findings also provide a strong foundation for future investigations to elucidate the precise mechanisms underlying their effects, paving the way for their potential clinical application.

Author agreement statement

We the undersigned declare that this manuscript is original, has not been published before and is not currently being considered for publication elsewhere. We confirm that the manuscript has been read and approved by all named authors and that there are no other persons who satisfied the criteria for authorship but are not listed. We further confirm that the order of authors listed in the manuscript has been approved by all of us. We understand that the Corresponding Author is the sole contact for the Editorial process. He is responsible for communicating with the other authors about progress, submissions of revisions and final approval of proofs.

Funding

PW is supported by the National Health and Medical Research Council (NHMRC) Ideas grant (APP 202934).

CRediT authorship contribution statement

Mehedi Hasan Bappi: Writing – review & editing, Formal analysis. **Islam Md. Zohorul:** Writing – review & editing, Software, Formal

analysis. **Phurpa Wangchuk:** Writing – review & editing, Supervision, Resources, Investigation, Funding acquisition, Conceptualization. **Subir Sarker:** Writing – review & editing, Supervision, Software, Resources, Project administration, Methodology, Investigation, Funding acquisition, Data curation, Conceptualization. **Rahaman Md. Mizanur:** Writing – original draft, Visualization, Validation, Methodology, Investigation, Formal analysis, Conceptualization. **Karma Yeshe:** Writing – review & editing, Resources, Methodology, Investigation, Formal analysis.

Declaration of Competing Interest

Authors declare that they have no competing interest in the present work.

Acknowledgements

Sarker is the recipient of an Australian Research Council Discovery Early Career Researcher Award (grant number DE200100367) funded by the Australian Government. The Australian Government had no role in the study design, data collection and analysis, decision to publish, or preparation of the manuscript.

Ethics approval and consent to participate

All ethical guidelines were followed as instructed by the JCU Ethics Committee, in accordance with the Australian Code for the Care and Use of Animals for Scientific Purposes. Ethical approval number for this work is JCU-IBC-240531–71. Additionally, requirement by the Queensland Biodiscovery Act 2004 (part 5 and section 14), this research was undertaken under an approved Biodiscovery Plan (Approval # CTS 07201/20) and Collection Authority (BCA20–002698).

Appendix A. Supporting information

Supplementary data associated with this article can be found in the online version at doi:10.1016/j.micres.2025.128343.

Data availability

The accession number has been included in the manuscript.

References

- Abdulqadir, R., Engers, J., Al-Sadi, R., 2023. Role of bifidobacterium in modulating the intestinal epithelial tight junction barrier: current knowledge and perspectives. *Curr. Dev. Nutr.*, 102026.
- Adolph, T.E., Meyer, M., Schwärzler, J., Mayr, L., Grabherr, F., Tilg, H., 2022. The metabolic nature of inflammatory bowel diseases. *Nat. Rev. Gastroenterol. Hepatol.* 19 (12), 753–767.
- Atreya, R., Neurath, M.F., 2005. Involvement of IL-6 in the pathogenesis of inflammatory bowel disease and colon cancer. *Clin. Rev. Allergy Immunol.* 28, 187–195.
- Bappi, M.H., Mia, M.N., Ansari, S.A., Ansari, I.A., Prottoy, A.A.S., Akbor, M.S., El-Nashar, H.A., El-Shazly, M., Mubarak, M.S., Torekul Islam, M., 2024. Quercetin increases the antidepressant-like effects of sclareol and antagonizes diazepam in thiopental sodium-induced sleeping mice: a possible GABAergic transmission intervention. *Phytother. Res.* 38 (5), 2198–2214.
- Bergmann, K.R., Liu, S.X., Tian, R., Kushnir, A., Turner, J.R., Li, H.-L., Chou, P.M., Weber, C.R., De Plaen, I.G., 2013. Bifidobacteria stabilize claudins at tight junctions and prevent intestinal barrier dysfunction in mouse necrotizing enterocolitis. *Am. J. Pathol.* 182 (5), 1595–1606.
- Bevins, C.L., Salzman, N.H., 2011. Paneth cells, antimicrobial peptides and maintenance of intestinal homeostasis. *Nat. Rev. Microbiol.* 9 (5), 356–368.
- Britton, G.J., Contijoch, E.J., Mogno, I., Vennaro, O.H., Llewellyn, S.R., Ng, R., Li, Z., Mortha, A., Merad, M., Das, A., 2019. Microbiotas from humans with inflammatory bowel disease alter the balance of gut Th17 and ROR γ t+ regulatory t cells and exacerbate colitis in mice. *Immunity* 50 (1), 212–224 e4.
- Caenepeel, C., Sadat Seyed Tabib, N., Vieira-Silva, S., Vermeire, S., 2020. How the intestinal microbiota May reflect disease activity and influence therapeutic outcome in inflammatory bowel disease. *Aliment. Pharmacol. Ther.* 52 (9), 1453–1468.

- Caetano, M.A.F., Castelucci, P., 2022. Role of short chain fatty acids in gut health and possible therapeutic approaches in inflammatory bowel diseases. *World J. Clin. Cases* 10 (28), 9985.
- Callahan, B.J., McMurdie, P.J., Rosen, M.J., Han, A.W., Johnson, A.J.A., Holmes, S.P., 2016. DADA2: High-resolution sample inference from illumina amplicon data. *Nat. Methods* 13 (7), 581–583.
- Chang, J.T., 2020. Pathophysiology of inflammatory bowel diseases. *N. Engl. J. Med.* 383 (27), 2652–2664.
- Chen, S., Zhao, H., Cheng, N., Cao, W., 2019. Rape bee pollen alleviates dextran sulfate sodium (DSS)-induced colitis by neutralizing IL-1 β and regulating the gut microbiota in mice. *Food Res. Int.* 122, 241–251.
- Chen, S., Wu, X., Tang, S., Yin, J., Song, Z., He, X., Yin, Y., 2021. Eugenol alleviates dextran sulfate sodium-induced colitis independent of intestinal microbiota in mice. *J. Agric. Food Chem.* 69 (36), 10506–10514.
- Clevers, H.C., Bevins, C.L., 2013. Paneth cells: maestros of the small intestinal crypts. *Annu. Rev. Physiol.* 75 (1), 289–311.
- Cohen, L.J., Cho, J.H., Gevers, D., Chu, H., 2019. Genetic factors and the intestinal microbiome guide development of microbe-based therapies for inflammatory bowel diseases. *Gastroenterology* 156 (8), 2174–2189.
- Cole, J.R., Wang, Q., Fish, J.A., Chai, B., McGarrell, D.M., Sun, Y., Brown, C.T., Porras-Alfaro, A., Kuske, C.R., Tiedje, J.M., 2014. Ribosomal database project: data and tools for high throughput rRNA analysis. *Nucleic Acids Res.* 42 (D1), D633–D642.
- Daina, A., Michielin, O., Zoete, V., 2019. SwissTargetPrediction: updated data and new features for efficient prediction of protein targets of small molecules. *Nucleic Acids Res.* 47 (W1), W357–W364.
- DeLano, W.L., 2002. Pymol: an open-source molecular graphics tool. *CCP4 Newsl. Protein Crystallogr* 40 (1), 82–92.
- Devika, N., Raman, K., 2019. Deciphering the metabolic capabilities of bifidobacteria using genome-scale metabolic models. *Sci. Rep.* 9 (1), 18222.
- Dieleman, Palmen, Akol, Bloemena, PEÑA, Meuwissen, Rees, V., 1998. Chronic experimental colitis induced by dextran sulphate sodium (DSS) is characterized by Th1 and Th2 cytokines. *Clin. Exp. Immunol.* 114 (3), 385–391.
- Douglas, G.M., Maffei, V.J., Zaneveld, J.R., Yurgel, S.N., Brown, J.R., Taylor, C.M., Huttenhower, C., Langille, M.G., 2020. PICRUST2 for prediction of metagenome functions. *Nat. Biotechnol.* 38 (6), 685–688.
- Fujio, K., Okamura, T., Yamamoto, K., 2010. The family of IL-10-secreting CD4+ t cells. *Adv. Immunol.* 105, 99–130.
- Fukuda, S., Toh, H., Hase, K., Oshima, K., Nakanishi, Y., Yoshimura, K., Tobe, T., Clarke, J.M., Topping, D.L., Suzuki, T., 2011. Bifidobacteria can protect from enteropathogenic infection through production of acetate. *Nature* 469 (7331), 543–547.
- Gavini, F., Van Esbroeck, M., Touzel, J., Fourment, A., Goossens, H., 1996. Detection of Fructose-6-phosphate phosphoketolase (F6PPK), a key enzyme of the Bifid-Shunt, in *ingardnerella vaginalis*. *Anaerobe* 2 (3), 191–193.
- Gong, S., Zheng, J., Zhang, J., Wang, Y., Xie, Z., Wang, Y., Han, J., 2022. Taxifolin ameliorates lipopolysaccharide-induced intestinal epithelial barrier dysfunction via attenuating NF- κ B/MLCK pathway in a Caco-2 cell monolayer model. *Food Res. Int.* 158, 111502.
- Grigor'eva, I.N., 2020. Gallstone disease, obesity and the firmicutes/bacteroidetes ratio as a possible biomarker of gut dysbiosis. *J. Pers. Med.* 11 (1), 13.
- Guo, M., Li, Z., 2019. Polysaccharides isolated from *nostoc commune* vaucher inhibit colitis-associated colon tumorigenesis in mice and modulate gut microbiota. *Food Funct.* 10 (10), 6873–6881.
- Health, A.G.Do, 2019. Inflammatory bowel disease. *Natl. Action Plan* 1, 1–28.
- Hur, S.J., Kang, S.H., Jung, H.S., Kim, S.C., Jeon, H.S., Kim, I.H., Lee, J.D., 2012. Review of natural products actions on cytokines in inflammatory bowel disease. *Nutr. Res.* 32 (11), 801–816.
- Huttenhower, C., Kostic, A.D., Xavier, R.J., 2014. Inflammatory bowel disease as a model for translating the microbiome. *Immunity* 40 (6), 843–854.
- Ihara, S., Hirata, Y., Koike, K., 2017. TGF- β in inflammatory bowel disease: a key regulator of immune cells, epithelium, and the intestinal microbiota. *J. Gastroenterol.* 52, 777–787.
- Islam, M.T., Bhuia, M.S., Sheikh, S., Hasan, R., Bappi, M.H., Chowdhury, R., Ansari, S.A., Islam, M.A., Saifuzzaman, M., 2024. Sedative effects of daidzin, possibly through the GABAA receptor interaction pathway: in vivo approach with molecular dynamic simulations. *J. Mol. Neurosci.* 74 (3), 83.
- Jabi, B., Mukherjee, R.K., Pimpalshende, P.M., Prajapati, B., Mishra, S., Srivastava, S., Maurya, U.S., Shahare, H.V., 2024. Synthesis, characterization, predicted adme value and molecular docking of vanadium containing metal complexes as potential antimicrobial activity. *Bull. Pure Appl. Sci. Zool.* 548–564.
- Jia, Q., Fang, S., Yang, R., Ling, Y., Mehmood, S., Ni, H., Gao, Q., 2024. Genistein alleviates dextran sulfate sodium-induced colitis in mice through modulation of intestinal microbiota and macrophage polarization. *Eur. J. Nutr.* 1–12.
- Jumper, J., Evans, R., Pritzel, A., Green, T., Figurnov, M., Ronneberger, O., Tunyasuvunakool, K., Bates, R., Zidek, A., Potapenko, A., 2021. Highly accurate protein structure prediction with AlphaFold. *nature* 596 (7873), 583–589.
- Knowler, S.A., Shindler, A., Wood, J.L., Lakkavaram, A., Thomas, C.J., de Koning-Ward, T.F., Hill-Yardin, E.L., Carvalho, T.G., Franks, A.E., 2023. Altered gastrointestinal tract structure and microbiome following cerebral malaria infection. *Parasitol. Res.* 122 (3), 789–799.
- Kobayashi, T., Okamoto, S., Hisamatsu, T., Kamada, N., Chinen, H., Saito, R., Kitazume, M.T., Nakazawa, A., Sugita, A., Koganei, K., 2008. IL23 differentially regulates the Th1/Th17 balance in ulcerative colitis and Crohn's disease. *Gut* 57 (12), 1682–1689.
- Kolde R. pheatmap: Pretty Heatmaps version 1.0. 12 from CRAN, 2019.
- Kostic, A.D., Xavier, R.J., Gevers, D., 2014. The microbiome in inflammatory bowel disease: current status and the future ahead. *Gastroenterology* 146 (6), 1489–1499.
- Krigul, K.L., Aasmets, O., Lüll, K., Org, T., Org, E., 2021. Using fecal immunochemical tubes for the analysis of the gut microbiome has the potential to improve colorectal cancer screening. *Sci. Rep.* 11 (1), 19603.
- Berkel K.V. The role of microbiota derived peptidoglycan fragments in diseases and therapies 2023.
- Langille, M.G., Zaneveld, J., Caporaso, J.G., McDonald, D., Knights, D., Reyes, J.A., Clemente, J.C., Burkepile, D.E., Vega Thurber, R.L., Knight, R., 2013. Predictive functional profiling of microbial communities using 16S rRNA marker gene sequences. *Nat. Biotechnol.* 31 (9), 814–821.
- Li, M.O., Flavell, R.A., 2008. Contextual regulation of inflammation: a duet by transforming growth factor- β and interleukin-10. *Immunity* 28 (4), 468–476.
- Li, M.O., Wan, Y.Y., Sanjabi, S., Robertson, A.-K.L., Flavell, R.A., 2006. Transforming growth factor- β regulation of immune responses. *Annu. Rev. Immunol.* 24 (1), 99–146.
- Liu, Y., Yang, X., Gan, J., Chen, S., Xiao, Z.-X., Cao, Y., 2022. CB-Dock2: improved protein-ligand blind docking by integrating cavity detection, docking and homologous template fitting. *Nucleic Acids Res.* 50 (W1), W159–W164.
- Lo Sasso, G., Khachatryan, L., Kondylis, A., Battey, J.N., Sierro, N., Danilova, N.A., Grigoryeva, T.V., Markelova, M.I., Khushnutdinova, D.R., Laikov, A.V., 2021. Inflammatory bowel disease-associated changes in the gut: focus on kazán patients. *Inflamm. Bowel Dis.* 27 (3), 418–433.
- Lofst Jr, E.V., Sandborn, W.J., 2002. Epidemiology of inflammatory bowel disease. *Gastroenterol. Clin. North Am.* 31 (1), 1–20.
- Love, M.L., Huber, W., Anders, S., 2014. Moderated estimation of fold change and dispersion for RNA-seq data with DESeq2. *Genome Biol.* 15, 1–21.
- Matchado, M.S., Rühlmann, M., Reitemeier, S., Kacprowski, T., Frost, F., Haller, D., Baumbach, J., List, M., 2024. On the limits of 16S rRNA gene-based metagenome prediction and functional profiling. *Microb. Genom.* 10 (2), 001203.
- Matsumoto, S., Hara, T., Nagaoka, M., Mike, A., Mitsuyama, K., Sako, T., Yamamoto, M., Kado, S., Takada, T., 2009. A component of polysaccharide peptidoglycan complex on *lactobacillus* induced an improvement of murine model of inflammatory bowel disease and colitis-associated cancer. *Immunology* 128 (1pt2), e170–e180.
- McMurdie, P.J., Holmes, S., 2013. Phyloseq: an r package for reproducible interactive analysis and graphics of microbiome census data. *PLoS One* 8 (4), e61217.
- Michaudel, C., Danne, C., Agus, A., Magniez, A., Aucouturier, A., Spatz, M., Lefevre, A., Kirchgessner, J., Rolhion, N., Wang, Y., 2023. Rewiring the altered tryptophan metabolism as a novel therapeutic strategy in inflammatory bowel diseases. *Gut* 72 (7), 1296–1307.
- Moore, K.W., de Waal Malefyt, R., Coffman, R.L., O'Garra, A., 2001. Interleukin-10 and the interleukin-10 receptor. *Annu. Rev. Immunol.* 19 (1), 683–765.
- Neurath, M.F., 2014. Cytokines in inflammatory bowel disease. *Nat. Rev. Immunol.* 14 (5), 329–342.
- Neurath, M.F., 2019. Targeting immune cell circuits and trafficking in inflammatory bowel disease. *Nat. Immunol.* 20 (8), 970–979.
- Ng, S.C., Shi, H.Y., Hamidi, N., Underwood, F.E., Tang, W., Benchimol, E.I., Panaccione, R., Ghosh, S., Wu, J.C., Chan, F.K., 2017. Worldwide incidence and prevalence of inflammatory bowel disease in the 21st century: a systematic review of population-based studies. *Lancet* 390 (10114), 2769–2778.
- O'garra Avieira, P., 2004. Regulatory t cells and mechanisms of immune system control. *Nat. Med.* 10 (8), 801–805.
- O'Leary, N.A., Wright, M.W., Brister, J.R., Ciufu, S., Haddad, D., McVeigh, R., Rajput, B., Robbette, B., Smith-White, B., Ako-Adjei, D., 2016. Reference sequence (RefSeq) database at NCBI: current status, taxonomic expansion, and functional annotation. *Nucleic Acids Res.* 44 (D1), D733–D745.
- Parada Venegas, D., De la Fuente, M.K., Landskron, G., González, M.J., Quera, R., Dijkstra, G., Harmsen, H.J., Faber, K.N., Hermoso, M.A., 2019. Short chain fatty acids (SCFAs)-mediated gut epithelial and immune regulation and its relevance for inflammatory bowel diseases. *Front. Immunol.* 10, 277.
- Paramsothy, S., Kamm, M.A., Kaakoush, N.O., Walsh, A.J., van den Bogaerde, J., Samuel, D., Leong, R.W., Connor, S., Ng, W., Paramsothy, R., 2017. Multidonor intensive faecal microbiota transplantation for active ulcerative colitis: a randomised placebo-controlled trial. *Lancet* 389 (10075), 1218–1228.
- Parks, D.H., Chuvochina, M., Rinke, C., Mussig, A.J., Chaumeil, P.-A., Hugenholtz, P., 2022. GTDB: an ongoing census of bacterial and archaeal diversity through a phylogenetically consistent, rank normalized and complete genome-based taxonomy. *Nucleic Acids Res.* 50 (D1), D785–D794.
- Peng, Y., Yan, Y., Wan, P., Chen, D., Ding, Y., Ran, L., Mi, J., Lu, L., Zhang, Z., Li, X., 2019. Gut microbiota modulation and anti-inflammatory properties of anthocyanins from the fruits of *lycium ruthenicum* Murray in dextran sodium sulfate-induced colitis in mice. *Free Radic. Biol. Med.* 136, 96–108.
- Pokusaeva, K., Fitzgerald, G.F., van Sinderen, D., 2011. Carbohydrate metabolism in bifidobacteria. *Genes Nutr.* 6, 285–306.
- Pyclik, M., Srutkova, D., Schwarzer, M., Gorska, S., 2020. Bifidobacteria cell wall-derived exo-polysaccharides, lipoteichoic acids, peptidoglycans, polar lipids and proteins—their chemical structure and biological attributes. *Int. J. Biol. Macromol.* 147, 333–349.
- Quast, C., Pruesse, E., Yilmaz, P., Gerken, J., Schweer, T., Yarza, P., Peplies, J., Glöckner, F.O., 2012. The SILVA ribosomal RNA gene database project: improved data processing and web-based tools. *Nucleic Acids Res.* 41 (D1), D590–D596.
- Rahaman, M.M., Wangchuk, P., Sarker, S., 2025. A systematic review on the role of gut microbiome in inflammatory bowel disease: spotlight on virome and plant metabolites. *Microb. Pathog.*, 107608.
- Ritmeijer, E., Ryan, R.Y., Byatt, B.J., Peck, Y., Yeshi, K., Daly, N.L., Zhao, G., Crayn, D., Loukas, A., Pyne, S.G., 2022. Anti-inflammatory properties of novel galloyl

- glucosides isolated from The Australian tropical plant uromyrtus metrosideros. *Chem. Biol. Interact.* 368, 110124.
- Sela, D.A., Chapman, J., Adeuya, A., Kim, J.H., Chen, F., Whitehead, T.R., Lapidus, A., Rokhsar, D., Lebrilla, C., German, J., 2008. The genome sequence of bifidobacterium longum subsp. Infantis reveals adaptations for milk utilization within the infant microbiome. *Proc. Natl. Acad. Sci.* 105 (48), 18964–18969.
- Shivanika, C., Kumar, D., Ragunathan, V., Tiwari, P., Sumitha, A., 2020. Molecular docking, validation, dynamics simulations, and pharmacokinetic prediction of natural compounds against the SARS-CoV-2 main-protease. *J. Biomol. Struct. Dyn.* 1. Song, F., Kuehl, J.V., Chandran, A., Arkin, A.P., 2021. A simple, cost-effective, and automation-friendly direct PCR approach for bacterial community analysis. *Msystems* 6 (5), 10.1128/msystems. 00224-21.
- Taleb, S., 2019. Tryptophan dietary impacts gut barrier and metabolic diseases. *Front. Immunol.* 10, 2113.
- Torres, J., Mehandru, S., Colombel, J.-F., Peyrin-Biroulet, L., 2017. Crohn's disease. *Lancet* 389 (10080), 1741–1755.
- Torres, M., Garcia-Martin, M., Fernandez, M., Nieto, N., Gil, A., Rios, A., 1999. Experimental colitis induced by trinitrobenzenesulfonic acid: an ultrastructural and histochemical study. *Dig. Dis. Sci.* 44 (12), 2523–2529.
- Waldner, M.J., Neurath, M.F., 2014. Master regulator of intestinal disease: IL-6 in chronic inflammation and cancer development. *Seminars immunology Elsevier* 26, 75–79.
- Waldschmitt, N., Kitamoto, S., Secher, T., Zacharioudaki, V., Boulard, O., Floquet, E., Delacre, M., Lamas, B., Pham, H.-P., Six, A., 2019. The regenerating family member 3 β instigates IL-17A-mediated neutrophil recruitment downstream of NOD1/2 signalling for controlling colonisation resistance independently of microbiota community structure. *Gut* 68 (7), 1190–1199.
- Wan, Y.Y.F., lavell, R.A., 2007. Yin–Yang' functions of transforming growth factor- β and t regulatory cells in immune regulation. *Immunol. Rev.* 220 (1), 199–213.
- Wangchuk, P., Navarro, S., Shepherd, C., Keller, P.A., Pyne, S.G., Loukas, A., 2015. Diterpenoid alkaloids of aconitum laciniatum and mitigation of inflammation by 14-O-acetylneoline in a murine model of ulcerative colitis. *Sci* 5 (1), 12845.
- Weersma, R.K., Zhernakova, A., Fu, J., 2020. Interaction between drugs and the gut microbiome. *Gut* 69 (8), 1510–1519.
- Wen, C., Chen, D., Zhong, R., Peng, X., 2024. Animal models of inflammatory bowel disease: category and evaluation indexes. *Gastroenterol. Rep.* 12, goae021.
- Wickham H., Wickham H., 2016. *Data analysis*, Springer.
- Wolber, G., Langer, T., 2005. LigandScout: 3-D pharmacophores derived from protein-bound ligands and their use as virtual screening filters. *J. Chem. Inf. Model.* 45 (1), 160–169.
- Wu, J., Wang, K., Wang, X., Pang, Y., Jiang, C., 2021. The role of the gut microbiome and its metabolites in metabolic diseases. *Protein Cell* 12 (5), 360–373.
- Wu, X.M., Tan, R.X., 2019. Interaction between gut microbiota and ethnomedicine constituents. *Nat. Prod. Rep.* 36 (5), 788–809.
- Xavier, R.J., Podolsky, D., 2007. Unravelling the pathogenesis of inflammatory bowel disease. *Nature* 448 (7152), 427–434.
- Yeshi, K., Ruscher, R., Hunter, L., Daly, N.L., Loukas, A., Wangchuk, P., 2020. Revisiting inflammatory bowel disease: pathology, treatments, challenges and emerging therapeutics including drug leads from natural products. *J. Clin. Med.* 9 (5), 1273.
- Yeshi, K., Jamtsho, T., Wangchuk, P., 2024. Current treatments, emerging therapeutics, and natural remedies for inflammatory bowel disease. *Molecules* 29 (16).
- Zhang, B., Gulati, A., Alipour, O., Shao, L., 2020. Relapse from deep remission after therapeutic de-escalation in inflammatory bowel disease: a systematic review and meta-analysis. *J. Crohn's. Colitis* 14 (10), 1413–1423.
- Zhang, M., Sun, K., Wu, Y., Yang, Y., Tso, P., Wu, Z., 2017. Interactions between intestinal microbiota and host immune response in inflammatory bowel disease. *Front. Immunol.* 8, 942.
- Zhang, Y., Thomas, J.P., Korcsmaros, T., Gul, L., 2024. Integrating multi-omics to unravel host-microbiome interactions in inflammatory bowel disease. *Cell Rep. Med.* 5 (9).
- Zhao, N., Yang, Y., Chen, C., Jing, T., Hu, Y., Xu, H., Wang, S., He, Y., Liu, E., Cui, J., 2022. Betaine supplementation alleviates dextran sulfate sodium-induced colitis via regulating the inflammatory response, enhancing the intestinal barrier, and altering gut microbiota. *Food Funct.* 13 (24), 12814–12826.